ISBN: 978-3-95450-227-1 ISSN: 2673-5490 doi:10.18429/JACoW-IPAC2022-WEPOMS011

SINGLE BUNCH INSTABILITY STUDIES WITH A NEW IMPEDANCE DATABASE FOR DIAMOND-II

Richard Fielder†, Hung-Chun Chao, Siwei Wang, Diamond Light Source, Oxfordshire, UK

Abstract

We present an updated impedance database for the Diamond-II storage ring [1], along with an analysis of single bunch instabilities and thresholds based on particle tracking simulations using Elegant [2]. Various cases with different chromaticity, insertion device parameters and harmonic cavity settings were studied, and the effects on the microwave instability, bunch lengthening and phase shifts were simulated and compared with analytic formulae. Preliminary results show that the single-bunch instability thresholds are above requirements for a uniform fill, and with inclusion of a harmonic cavity the longitudinal and transverse instability thresholds can also satisfy requirements for a hybrid fill.

INTRODUCTION

Single bunch dynamics are an important consideration for synchrotron light sources, since they place limits on the maximum bunch charge and hence total beam current. The instability thresholds are strongly influenced by impedance, as well as other factors such as chromaticity.

Diamond-II is planned to operate with two different fill patterns. The standard fill will have all bunches with equal charge, with 5 gaps of 7 buckets for ion clearing, giving four trains of 180 bunches and one of 179. A hybrid fill pattern providing a single high-charge bunch in addition to the main bunch train will also be offered. The details of the hybrid fill are still under study, but the target is to offer the same 3 nC bunch charge as is currently available at Diamond. This gives requirements for the instability thresholds of at least 0.33 mA per bunch in standard fill and 1.6 mA in hybrid fill. These requirements are shown as black dash-dotted lines on the relevant figures. It is planned to operate at a nominal chromaticity of [2] for the horizontal and vertical planes respectively.

We previously reported [3] on the production of an impedance database for Diamond-II using an Accelerator Toolbox-like structure [4]. This has since been updated with more detail and updated designs for some components. We present here an overview of the updated impedance database and results of single bunch effects comparing analytic formulae and particle tracking.

IMPEDANCE DATABASE

There are 252 BPMs in the Diamond-II lattice. Some are integrated into the large dipole vessel assemblies, while the rest incorporate flanges, bellows and tapers in addition to the BPM block itself. One dipole vessel includes a mirror inserted horizontally for the visible light extraction system. The RF cavities remain the largest contributors to the longitudinal impedance.

Significant updated components include the collimators, three in each plane with a nominal gap of ±3.5 mm for the horizontal and ±1.5 mm for the vertical. Injection striplines and diagnostic screens have also been added. The contributions to the resistive wall impedance have also been updated, with the new values shown in Table 1.

Figure 1 shows the real and imaginary impedance in each plane calculated for a 3 mm sigma Gaussian bunch and weighted by the local beta function for each component, comparing the cases with IDs and collimators all fully open, and with IDs closed to minimum gaps and collimators at nominal gaps. The main contributions are highlighted separately for each plane, with the remaining components grouped as “other”.

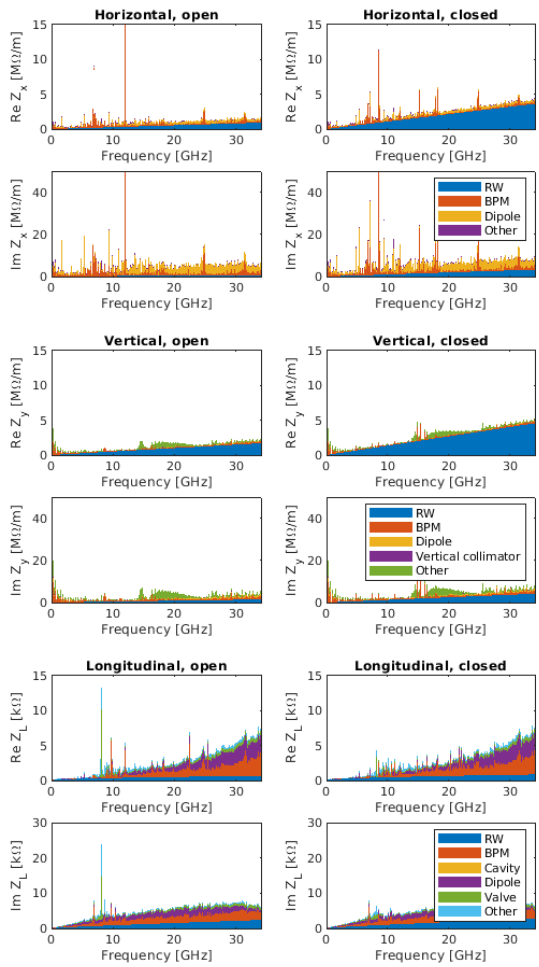

Figure 1: Real and imaginary impedance for Diamond-II with main contributions highlighted in each plane, with IDs and collimators open (left) and closed (right). Top: horizontal, middle: vertical, bottom: longitudinal.

† richard.fielder@diamond.ac.uk

ISBN: 978-3-95450-227-1 ISSN: 2673-5490 doi:10.18429/JACoW-IPAC2022-WEPOMS011

The effective longitudinal impedance is given by

$$\left(\frac{Z_\parallel}{n}\right)_{\text{eff}} = \frac{\int_{-\infty}^{\infty} \frac{Z_\parallel(\omega)\omega_0}{\omega} h(\omega)d\omega}{\int_{-\infty}^{\infty} h(\omega)d\omega},$$

where $Z_\parallel(\omega)$ is the longitudinal impedance and h(ω) the bunch power spectrum. The effective transverse impedance can then be calculated by

$$(Z_\perp)_{\text{eff}} = \frac{\int_{-\infty}^{\infty} Z_\perp(\omega)h(\omega)d\omega}{\int_{-\infty}^{\infty} h(\omega)d\omega}.$$

A summary of the effective impedance for each plane is shown in Table 2.

Table 1: Summary of Resistive Wall Parameters in Diamond-II. Multi-layer Materials Show Values for the Coating Followed by the Underlying Bulk Material

Material	Length (m)	Conductivity (S/m)
Steel	42.02	1.35 e6
Copper	51.85	5.96 e7
Aluminium	96.00	3.77 e7
NEG-coated copper	336.36	1.00 e5, 5.96 e7
NEG-coated aluminium	31.73	1.00 e5, 3.77 e7
Ti-coated alumina	2.60	2.38 e6, 0.00
Total	560.56	

Table 2: Effective Impedance in Each Plane with All IDs Open or Closed

	Longitudinal (Ω)	Horizontal (MΩ/m)	Vertical (MΩ/m)
IDs open	0.2044	1.10	1.19
IDs closed	0.2166	2.57	2.91

SINGLE BUNCH EFFECTS

Single bunch instabilities have been studied both analytically and with tracking in Elegant using a one-turn map and lumped impedance model. Studies have also been carried out including a harmonic cavity set to flat-potential conditions [5] to be able to scan different bunch currents.

Phase Shift

The shift of the synchronous phase, bunch lengthening and microwave instability threshold when including the longitudinal impedance have been calculated for different bunch currents up to 5 mA with a step of 0.25 mA. The phase shift from the tracking result is plotted in Fig. 2 and compared to the analytic formula [6]

$$\Delta\phi_s = \frac{I_b k_\parallel}{f_0 V_{\text{rf}} \cos\phi_s},$$

where f_0 is the revolution frequency, V_{rf} the RF voltage, ϕ_s the synchronous phase and $k_\parallel$ the loss factor expressed by

$$k_\parallel = \frac{1}{2\pi}\int_{-\infty}^{\infty} Z_\parallel(\omega)h(\omega)d\omega,$$

Without the harmonic cavity, the phase shift calculated from the formula matches well with the tracking result up to the point where the bunch profile starts to deviate too much from a Gaussian due to potential well distortion. The harmonic cavity increases the phase shift as expected due to the smaller RF focusing provided by the flat potential well.

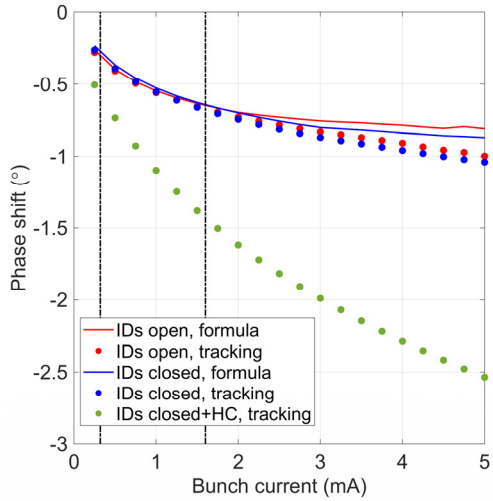

Figure 2: Synchronous phase shift due to longitudinal impedance.

Bunch Lengthening

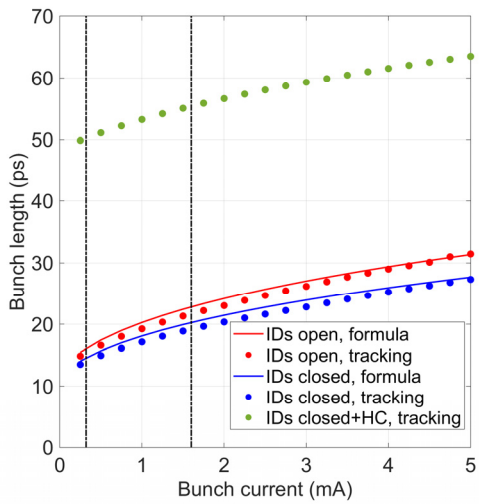

Figure 3: Bunch lengthening with current including longitudinal impedance.

Figure 3 shows the bunch lengthening with current from tracking and analytically using the modified Zotter's formula [7]

$$\left(\frac{\sigma_t}{\sigma_{t0}}\right)^3 - \frac{\sigma_t}{\sigma_{t0}} = \frac{I_b \alpha_c e}{4\sqrt{\pi} v_s^2 \omega_0^3 \sigma_{t0}^3 E} \text{Im}\left(\frac{Z_\parallel}{n}\right)_{\text{eff}},$$

where σ_{t0} is the zero current bunch length, I_b the bunch current, α_c the momentum compaction factor, e the electron charge, ν_s the synchrotron tune, ω_0 the angular revolution frequency, E the beam energy and $(Z_\parallel/n)_{\text{eff}}$ the effective

ISBN: 978-3-95450-227-1 ISSN: 2673-5490 doi:10.18429/JACoW-IPAC2022-WEPOMS011

longitudinal impedance. Tracking results differ slightly from the analytic since the true bunch profile is non-Gaussian.

Energy Spread

The energy spread is shown in Fig. 4. The microwave instability threshold is estimated to be the bunch current above which the energy spread grows by more than 1% above its natural value, which gives a threshold of 2 mA for the bare lattice and 2.5 mA for the lattice with closed IDs. The harmonic cavity increases the threshold to above 5 mA. The calculated microwave instability threshold is above the foreseen operational current requirements for both the standard and the hybrid mode.

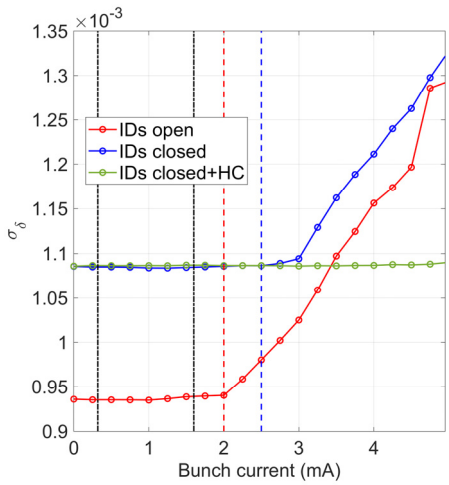

Figure 4: Energy spread with current including longitudinal impedance. The dashed red and blue lines show the estimated microwave instability threshold.

Tune Shift

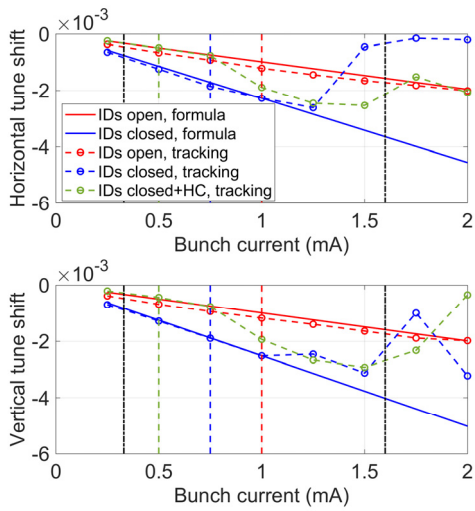

Figure 5: Betatron tune shift at zero chromaticity. Horizontal (top), vertical (bottom). The coloured dashed lines show the corresponding TMCI thresholds from tracking.

The tune shift at zero chromaticity as function of bunch current is shown in Fig. 5. The tune shift from tracking has been compared to the analytic formula [8]

$$\frac{d\Omega}{dI} = -\frac{\beta \mathrm{Im}(Z_\perp)_{\mathrm{eff}}}{\frac{4\sqrt{\pi}\sigma_t E}{e}}$$

using the bunch length obtained from tracking, where β is the average beta function. In our calculation, the average beta function is replaced by the local beta functions when calculating the lumped impedance. The transverse mode coupling instability occurs when the frequency of mode 0 and mode -1 merge, which happens when the tune shift of mode 0 and mode -1 roughly sums to the synchrotron tune. This is in reasonable agreement with the instability thresholds found from tracking (dashed lines in Fig. 5). As can be seen, below the threshold the tune decreases linearly with bunch current.

Head-Tail Instability

The thresholds for head-tail instabilities at different chromaticities estimated by tracking is plotted in Fig. 6. As expected, higher chromaticity helps to increase the single-bunch current threshold. The harmonic cavity helps to increase the thresholds at non-zero chromaticity, but actually reduces the TMCI threshold. The results show that in both planes, when including the harmonic cavity, the instability threshold is larger than 4.5 mA for a chromaticity above 2. Without the harmonic cavity, 3.0 mA can be stored at the nominal chromaticity, which meets the operation requirement for both the standard and hybrid mode.

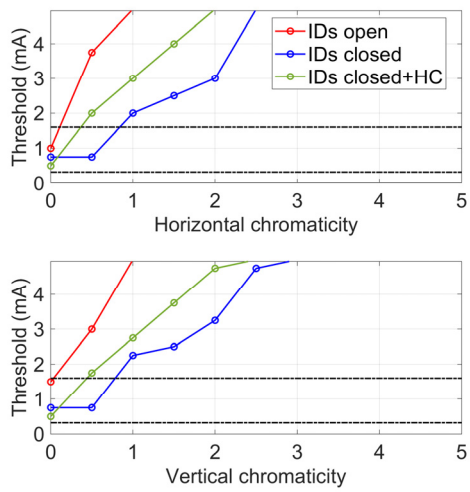

Figure 6: Transverse instability threshold vs. chromaticity. Horizontal (top), vertical (bottom).

CONCLUSIONS

The impedance database for Diamond-II has been updated, and the effects of the impedance on single bunch dynamics have been assessed, including bunch lengthening, phase shift, tune shift and instability thresholds. At the nominal chromaticity of 2 in both transverse planes, the microwave and head-tail instability thresholds have close to a factor 2 safety margin above the required currents even in the worst case with IDs closed, hybrid fill and no harmonic cavity.

ISBN: 978-3-95450-227-1 ISSN: 2673-5490 doi:10.18429/JACoW-IPAC2022-WEPOMS011

REFERENCES

[1] "Diamond-II Technical Design Report", Diamond Light Source, to be published, https://www.diamond.ac.uk/Home/About/Vision/Diamond-II.html

[2] M. Borland, "elegant: A Flexible SDDS-Compliant Code for Accelerator Simulation," Advanced Photon Source LS-287, September 2000.

[3] R. T. Fielder and T. Olsson, "Construction of an Impedance Model for Diamond-II", in *Proc. IPAC'21,* Campinas, Brazil, May 2021, pp. 455-458. doi:10.18429/JACoW-IPAC2021-MOPAB127

[4] A. Terebilo, "Accelerator toolbox for MATLAB". No. SLAC-PUB-8732. Stanford Linear Accelerator Center, Menlo Park, CA (US), 2001.

[5] T. Olsson and H. C. Chao, "Fill Pattern for Reducing Transient Beam Loading and Ion-Trapping in the Diamond-II Storage Ring", presented at the IPAC'22, Bangkok, Thailand, Jun. 2022, paper TUPOMS031, this conference.

[6] V. Smaluk, I. Martin, R. T. Fielder and R. Bartolini, "Beam-based model of broad-band impedance of the Diamond Light Source", *Phys. Rev. Spec. Top. Accel Beams*, vol. 18, no. 6, p. 064401, 2015. doi:10.1103/PhysRevSTAB.18.064401.

[7] A. Blednykh, G. Bassi, V. Smaluk and R. Lindberg, "Impedance modeling and its application to the analysis of the collective effects", *Phys. Rev. Accel. Beams*, vol. 24, no. 10, p.104801, 2021 doi:10.1103/PhysRevAccelBeams.24.104801.

[8] V. Smaluk, "Impedance computations and beam-based measurements: A problem of discrepancy", *Nucl. Instrum. Methods Phys. Res., Sect. A,* vol. 888, pp. 22-30, 2018. doi:10.1016/j.nima.2018.01.047